Journal of Thermal Analysis and Calorimetry, Vol. 72 (2003) 135–144

THERMAL DECOMPOSITION OF CHROMIUM(III) NITRATE(V) NANOHYDRATE

Different chromium oxides $CrO_{1.5+y}$ formation

A. Małecki[*], *B. Małecka, R. Gajerski and S. Łabuś*

University of Mining and Metallurgy, Faculty of Materials Science and Ceramics,
30 Mickiewicz Av., 30-059 Cracow, Poland

Abstract

Thermal decomposition of $Cr(NO_3)_3{\cdot}9H_2O$ in helium and in synthetic air was studied by means of TG, DTA, EGA and XRD analysis. The dehydration occurs together with decomposition of nitrate(V) groups. Eight distinct stages of reaction were found. Intermediate products of decomposition are hydroxy- and oxynitrates containing chromium in hexa- and trivalent states. The process carried out in helium leads to $Cr^{III}_{\sim 0.07}Cr^{VI}_{\sim 0.93}O_{\sim 2.90}$ at about 260°C and in air $Cr^{III}_{\sim 0.01}Cr^{VI}_{\sim 0.99}O_{\sim 2.99}$ is formed at about 200°C. The final product of decomposition (>450°C) is Cr_2O_3, both in helium and in air.

Keywords: chromium(III) nitrate(V), chromium oxides, evolved gas analysis, thermal decomposition

Introduction

Thermal decomposition of $Cr(NO_3)_3{\cdot}9H_2O$ was a subject of many investigations due to significant meaning of the final product of this reaction which generally can be described as nonstoichiometric $CrO_{1.5+y}$ [1–4]. Depending on the conditions of reaction (temperature, heating rate, mass of sample, surrounding atmosphere) thermal decomposition leads to chromium oxides with different ratio Cr:O, different size and porosity or specific area of the forming grains. All these factors are important from the point of view of the potential use of oxides (catalysers [5], gas-sensitive materials [6], powders for polishing etc.). The majority of papers related to $CrO_{1.5+y}$ properties is devoted to the problems concerning mobility of oxygen in this system ($CrO_{1.5+y} \leftrightarrow CrO_{1.5+y'} + O_2$) [7, 8]. The relations between degradation of nitrate(V) groups during thermal decomposition the $Cr(NO_3)_3{\cdot}9H_2O$ and the composition of $CrO_{1.5+y}$, being a product of chromium nitrate decomposition, remain still weakly recognized. Applying combined technique like evolved gas analysis together with thermogravimetry and differential thermal analysis gives extended possibilities for explaining these relations. In the present paper we are giving the complete description of thermal decomposition of $Cr(NO_3)_3{\cdot}9H_2O$ in helium and in air atmosphere and we indicate mentioned above relations between the conditions in which reaction proceeds and the composition of final product.

---

[*] Author for correspondence: E-mail: malecki@uci.agh.edu.pl

1388–6150/2003/ $ 20.00

Akadémiai Kiadó, Budapest
Kluwer Academic Publishers, Dordrecht

Experimental

In all the measurements a commercial, pure for analysis, $Cr(NO_3)_3{\cdot}9H_2O$ (POCh, Gliwice, Poland) has been used. Chemical analysis showed that the real composition of this compound was $Cr(NO_3)_3{\cdot}({\sim}9.2)H_2O$. Thermal decomposition of $Cr(NO_3)_3{\cdot}9H_2O$ was studied using simultaneous TG/DTA apparatus (SDT 2960 TA Instruments) connected on-line with quadrupole mass spectrometer (QMD 300, ThermoStar, Balzers, Lichtenstein). The phase composition of partial and final products of decomposition were studied by XRD analysis using Siemens D5005 (Bruker-AXS, Germany) apparatus (radiation CuK_α and graphite monochromator). The mass of samples, placed in platinium crucibles (120 mg), was 15±1 mg. The tentative measurements confirmed that the way of decomposition is mass independent when sample mass is lower than 20 mg. The heating rates applied were 0.5–10°C min^{-1}. Decomposition was carried out in helium or synthetic air (flow rate 6 dm^3 h^{-1} through chamber of 60 cm^3 volume). During thermal decomposition the chemical composition of gaseous products of the reaction was determined by mass spectrometry (EGA). Ionic currents corresponding to M/q (M – molecular mass, q – charge of ion in electron charge units) equal to 16 (O^+), 17 (HO^+), 18 (H_2O^+), 28 (N_2^+), 30 (NO^+), 32 (O_2^+), 46 (NO_2^+) and 63 (HNO_3^+) were detected.

Results and discussion

The course of thermal decomposition of $Cr(NO_3)_3{\cdot}9H_2O$ strongly depends on the conditions in which reaction proceeds. The most important role plays the mass of sample

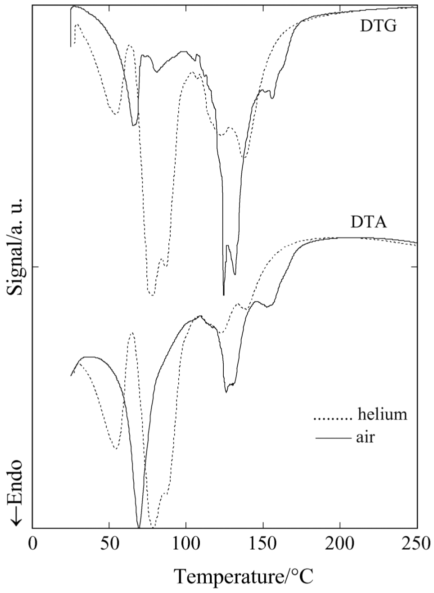

Fig. 1 Thermal decomposition of $Cr(NO_3)_3{\cdot}9H_2O$ in helium and in air (temperature <250°C, heating rate 2.5°C min^{-1})

and atmosphere surrounding decomposing sample [9]. As a matter of fact, discrepancies between authors of earlier reports result from differences in experimental conditions. Performing our experiments we spent a lot of time to determine conditions at which general picture of reaction studied becomes independent on secondary factors such as mass sample or gas flow rate. Figures 1 and 2 present DTA and DTG curves of thermal decomposition of $Cr(NO_3)_3{\cdot}(\sim 9)H_2O$ obtained at heating rate 2.5 K min^{-1} in helium and air atmospheres. Figure 1 is plotted for the temperature region below 250°C corresponding to degradation of NO_3^- groups, and Fig. 2 describes the second temperature region (>350°C), related to oxygen removal from Cr–O system, which was formed after NO_3^- decomposition. It is easy to notice, that especially in the final stages of decomposition, the differences between decomposition of $Cr(NO_3)_3{\cdot}9H_2O$ in helium and in air are significant. In Figs 3 and 4 the results of EGA analysis for reaction performed in helium and in air, respectively, are given.

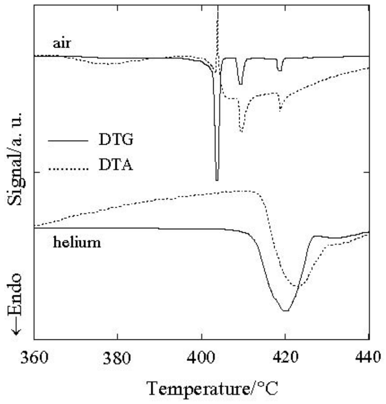

Fig. 2 Thermal decomposition of $Cr(NO_3)_3{\cdot}9H_2O$ in helium and in air (temperature <350°C, heating rate 2.5°C min^{-1})

Let us assume that area under $I_{M/q}(T)$ curve (where $I_{M/q}(T)$ is ionic current corresponding to ions with indicated M/q value) is related to the total amount of gas product identified by M/q value (for example M/q=30 corresponds to NO^+). Now it is possible to determine degree of decomposition $\alpha_{M/q}(T)$ as a function of temperature T, in respect to the particular product of decomposition, according to the following definition:

$$\alpha_{M/q}(T)=\frac{\int_0^{T} TI_{M/q}(T)\mathrm{d}T}{\int_0^{T_k} TI_{M/q}(T)\mathrm{d}T}$$

where T_k is temperature at which gaseous product with given M/q stops to evolve [10].

Figures 5 and 6 show values of $\alpha_{M/q}$ as a function of temperature calculated for $Cr(NO_3)_3{\cdot}9H_2O$ thermal decomposition in helium and in air atmosphere, respectively.

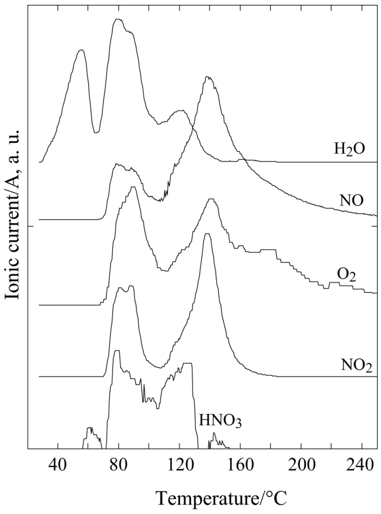

Fig. 3 Gaseous products of thermal decomposition of $Cr(NO_3)_3 \cdot 9H_2O$ in helium (heating rate 2.5°C min^{-1})

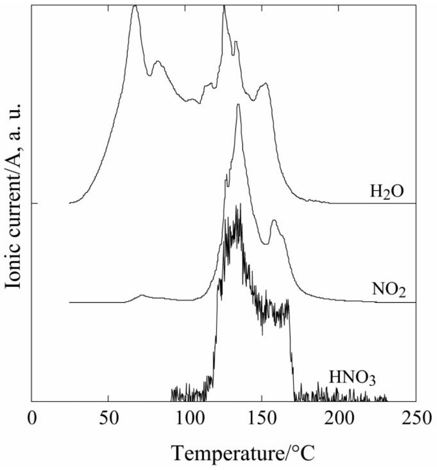

Fig. 4 Gaseous products of thermal decomposition of $Cr(NO_3)_3 \cdot 9H_2O$ in air (heating rate 2.5°C min^{-1})

In the case of measurements performed in air atmosphere, formation of NO is not observed due to secondary reaction $2NO+O_2=2NO_2$. $\alpha_{M/q=32}(T)$ corresponding to oxygen O_2 was not calculated for decomposition in air, because changes in total oxygen concentration in air due to decomposition of nitrate are negligible. The values of $\alpha_{M/q}$ are presented together with α_{TG} corresponding to the total change of mass during decomposition calculated on the basis of TG curve.

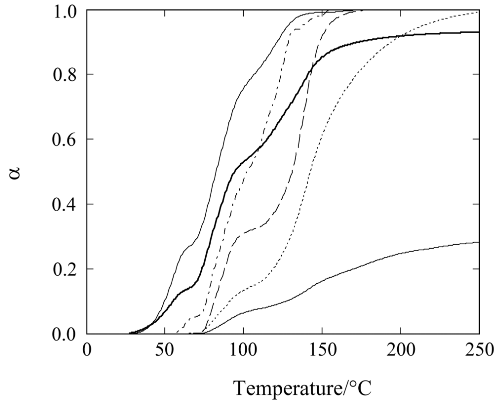

Fig. 5 Degree of decomposition of $Cr(NO_3)_3 \cdot 9H_2O$ in respect to different gaseous products (in helium, heating rate 2.5°C min^{-1})

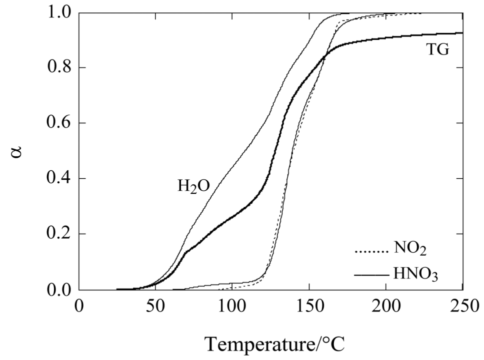

Fig. 6 Degree of decomposition of $Cr(NO_3)_3 \cdot 9H_2O$ in respect to different gaseous products (in air, 2.5°C min^{-1})

The detailed quantitative analysis of the results obtained shows, that in the case of $Cr(NO_3)_3 \cdot 9H_2O$ thermal decomposition is possible to distinguish eight stages of this reaction both in helium (*Ih–VIIIh*) and in air atmosphere (*Ia–VIIIa*). However stages denoted by *h* are not identical with corresponding stages denoted by *a*. Temperature ranges of these stages are not well separated and depend on heating rate and mass of the sample. This dependence becomes strong when mass of the sample exceeds 20 mg and heating rate is higher than 7–8°C min^{-1}. The description of reaction mechanism given below corresponds to heating rate 2.5°C min^{-1}. The limits of indicated temperature ranges for other heating rates, but lower than 8°C min^{-1}, can change by ±5°C.

Decomposition of $Cr(NO_3)_3 \cdot 9H_2O$ in helium

Stage *Ih*: <~55°C, $\alpha_{TG} \cong 0.1$

In this stage melting of sample (<50°C) and partial dehydration take place.

$$Cr(NO_3)_3\cdot(\sim9)H_2O \xrightarrow{<55^\circ C} Cr(NO_3)_3\cdot(\sim7.5)H_2O+(\sim1.5)H_2O \tag{1}$$

From Fig. 5 is seen that $\alpha_{M/q=18}$ reaches about 0.18. Relatively wide DTA signal with minimum in ~55°C (Fig. 1) corresponds to melting and water vaporization.

Stage *IIh*: ~55 – ~70°C, $\alpha_{TG}\cong0.15$

Ionic current corresponding M/q=63 (HNO_3) appears (Fig. 3). Dehydration continues but with significantly lower rate that results from combining hydration water into HNO_3 and hydroxynitrate:

$$Cr(NO_3)_3\cdot(\sim7.5)H_2O\rightarrow Cr(OH)_z(NO_3)_{3-z}\cdot(\sim6-z)H_2O+zHNO_3+(\approx1.5)H_2O \tag{2}$$

The detailed analysis of the values of ionic current corresponding to HNO_3 shows that amount of nitrogen, which is removed from reacting system in the form of HNO_3 during the whole process, does not exceed 5% of total nitrogen and decreases when heating rate becomes lower.

Stage *IIIh*: ~70 – ~110°C, $\alpha_{TG}\cong0.58$

Decomposition of nitrate(V) groups begins. Evolution of H_2O, HNO_3, NO, NO_2 and O_2 corresponding to reactions (3) and (4) is observed (Fig. 1 and Fig. 3):

$$Cr(OH)_z(NO_3)_{3-z}\cdot(\sim6-z)H_2O \xrightarrow{\sim70-110^\circ C}$$

$$Cr(OH)_{z+z'}(NO_3)_{3-z-z'}\cdot(\sim1.5-z')H_2O+z'HNO_3+(\sim4.5)H_2O \tag{3}$$

$$NO_3^-=xNO+(1-x)NO_2+\frac{2x+1}{4}O_2+\frac{1}{2}O^{2-} \tag{4}$$

Approximately 25% of total quantity of nitrogen removed in this stage is produced in reaction (4). Amount of oxygen formed in this stage in comparison with total loss of mass indicates, that simultaneously with reaction (4) oxidation of Cr^{3+} has to take place and ~75% of nitrogen removed is contained in NO and NO_2 produced in reaction (5):

$$Cr(OH)_z(NO_3)_{3-z}\cdot pH_2O \xrightarrow{70-110^\circ C}$$

$$Cr^{III}_{1-x}Cr^{VI}_xO_y(OH)_w(NO_3)_t\cdot p'H_2O+(HNO_3, NO, NO_2, O_2, H_2O) \tag{5}$$

At the end of stage *IIIh* ~45% of total amount of nitrogen and ~80% of total amount of H_2O are removed from decomposing sample.

Stage *IVh*: ~110 – ~170°C, $\alpha_{TG}\cong0.9$

The continuation of processes described by reaction (5) and formation of oxynitrates:

$$Cr^{III}_{1-x}Cr^{VI}_xO_y(OH)_w(NO_3)_t\cdot p'H_2O \xrightarrow{100-170^\circ C}$$

$$Cr^{III}_{1-x'}Cr^{VI}_{x'}O_{y'}(NO_3)_t+(NO, NO_2, O_2, H_2O) \tag{6}$$

At the end of this stage 100% of water and 90% of nitrogen is removed from decomposing sample. As it is seen on Fig. 5 at the end of this stage NO_2 evolution stops.

Stage *Vh*: ~160 – ~260°C, $\alpha_{TG}\cong0.92$

The residual nitrogen is removed from the sample only in form of NO (Fig. 5). The absence of water in gaseous products is the proof that oxynitrates actually form in the reaction (6).

$$Cr^{III}_{1-x'}Cr^{VI}_{x'}O_{y'}(NO_3)_{t'} \xrightarrow{160-260\,^{\circ}C} Cr^{III}_{\sim0.07}Cr^{VI}_{\sim0.93}O_{\sim2.90}+(NO,\ O_2) \qquad (7)$$

At the end of discussed stage decomposing sample is solid, practically insoluble in water. XRD analysis showed that oxide system $Cr^{III}_{\sim0.07}Cr^{VI}_{\sim0.93}O_{\sim2.90}$ is amorphous. It is worth noticing that composition of solid product of reaction (7) depends on heating rate. When heating rate changes from 2.5 to 8°C min^{-1} the composition of chromium oxide varies from $Cr^{III}_{\sim0.07}Cr^{VI}_{\sim0.93}O_{\sim2.90}$ to $Cr^{III}_{\sim0.15}Cr^{VI}_{\sim0.85}O_{\sim2.78}$.

Stage *VIh*: ~260 – ~400°C, $\alpha_{TG}\cong0.95$

$$Cr^{III}_{\sim0.07}Cr^{VI}_{\sim0.93}O_{\sim2.90} \xrightarrow{260-400\,^{\circ}C} Cr^{III}_{\sim0.2}Cr^{VI}_{\sim0.8}O_{\sim2.70}(+Cr_2O_3)+O_2 \qquad (8)$$

Slow evolution of oxygen (even in isothermal conditions) is observed. Above 300°C crystallization of the sample is noticed. The main XRD reflexes correspond to Cr_2O_3. During registration of XRD spectra in high temperature chamber small amount of unidentified CrO_z phase appeared (database PDF-2 ed. 1998 was checked). In some measurements small amounts of CrO_2 also seemed to be observed, nevertheless the CrO_2 formation is not always noticeable.

Stage *VIIh*: ~400 – ~428°C, $\alpha_{TG}\cong0.98$

$$Cr^{III}_{\sim0.2}Cr^{VI}_{\sim0.8}O_{\sim2.70}(+Cr_2O_3) \xrightarrow{400-428\,^{\circ}C} Cr^{III}_{\sim0.85}Cr^{VI}_{\sim0.15}O_{\sim1.70}(+Cr_2O_3)+O_2 \qquad (9)$$

In this stage fast oxygen evolution takes place (Fig. 7), phase CrO_z disappeared and relatively stable phase $Cr^{III}_{\sim0.85}Cr^{IV}_{\sim0.15}O_{\sim1.70}$ has formed. Only Cr_2O_3 structure is observed by XRD analysis.

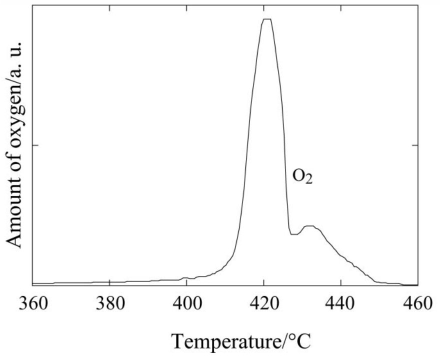

Fig. 7 Oxygen evolution during thermal decomposition of $Cr^{III}_{\sim0.2}Cr^{VI}_{\sim0.8}O_{\sim2.70}$ (in helium)

Stage *VIIIh*: ~428 – >500°C, (end of decomposition)

$$\mathrm{Cr}^{\mathrm{III}}_{\sim 0.85}\mathrm{Cr}^{\mathrm{VI}}_{\sim 0.15}\mathrm{O}_{\sim 1.70}(+\mathrm{Cr_2O_3}) \xrightarrow{>427^{\circ}\mathrm{C}} \mathrm{Cr_2O_3}+\mathrm{O_2} \tag{10}$$

Decomposition of $Cr(NO_3)_3 \cdot 9H_2O$ in air

Stage *Ia*: <~70°C, $\alpha_{\mathrm{TG}} \cong 0.15$

Reaction identical as in Stage *Ih* (Eq. (1)), but final temperature of this stage is about 15°C higher (Fig. 6).

Stage *IIa*: ~70 – ~95°C, $\alpha_{\mathrm{TG}} \cong 0.25$

$$\mathrm{Cr(NO_3)_3}\cdot(\approx 7.5)\mathrm{H_2O} \xrightarrow{<95^{\circ}\mathrm{C}} \mathrm{Cr(NO_3)_3}\cdot(\approx 5)\mathrm{H_2O}+(\approx 2.5)\mathrm{H_2O} \tag{11}$$

This stage is seen quite clearly on DTG curve (Fig. 1). Approximately 45% of total amount of water and <2% of NO_2 and HNO_3 are removed from decomposing system.

Stage *IIIa*: ~95 – ~150°C, $\alpha_{\mathrm{TG}} \cong 0.8$

In this stage the reactions occur corresponding to reactions in stages *IIIh* and *IVh*. At the end of this stage ~90% of water and ~70% of nitrogen is removed from decomposing sample (in the form of NO_2).

Stage *IVa*: ~150 – ~200°C, $\alpha_{\mathrm{TG}} \cong 0.9$

The reactions running in this stage are similar to those in stages *IVh* and *Vh* associated with secondary oxidation of NO to NO_2.

$$\mathrm{Cr(OH)_z(NO_3)_{3-z}}\cdot p'H_2\mathrm{O} \xrightarrow{150-200^{\circ}\mathrm{C},\ \mathrm{O_2}} \mathrm{Cr}^{\mathrm{III}}_{1-\mathrm{x}}\mathrm{Cr}^{\mathrm{VI}}_{\mathrm{x}}\mathrm{O_y(OH)_w(NO_3)_t}\cdot p''\mathrm{H_2O}+$$

$$+(\mathrm{HNO_3},\ \mathrm{NO_2},\ \mathrm{O_2},\ \mathrm{H_2O}) \tag{12}$$

$$\mathrm{Cr}^{\mathrm{III}}_{1-\mathrm{x'}}\mathrm{Cr}^{\mathrm{VI}}_{\mathrm{x'}}\mathrm{O}_{\mathrm{y'}}(\mathrm{NO_3})_{\mathrm{t'}} \xrightarrow{150-200^{\circ}\mathrm{C},\ \mathrm{O_2}} \mathrm{Cr}^{\mathrm{III}}_{\sim 0.01}\mathrm{Cr}^{\mathrm{VI}}_{\sim 0.99}\mathrm{O}_{\sim 2.99}+(\mathrm{NO_2},\ \mathrm{O_2}) \tag{13}$$

In Fig. 6 it is seen that degrees of evolution of NO_2 as well as HNO_3 as a function of temperature are very close. This suggests that instead reaction (12) the following reaction can take place:

$$\mathrm{Cr(OH)_z(NO_3)_{3-z}}\cdot p'\mathrm{H_2O} \xrightarrow{150-200^{\circ}\mathrm{C},\ \mathrm{O_2}} \mathrm{Cr}^{\mathrm{III}}_{\sim 0.01}\mathrm{Cr}^{\mathrm{VI}}_{\sim 0.99}\mathrm{O}_{\sim 2.99}+$$

$$+(\mathrm{HNO_3},\ \mathrm{NO_2},\ \mathrm{O_2},\ \mathrm{H_2O}) \tag{12a}$$

The chromium oxide phase obtained as a result of reaction (12a) or (13) has composition very close to CrO_3. Thus we can assume that external oxygen (from air) takes part in the reaction. The estimated error for chromium(VI) contents in the case of our experiment does not exceed 3%. Thus x' in the formula $\mathrm{Cr}^{\mathrm{III}}_{1-\mathrm{x'}}\mathrm{Cr}^{\mathrm{VI}}_{\mathrm{x'}}\mathrm{O}_{1.5+1.5\mathrm{x'}}$ has to be greater than 0.97. Nevertheless decomposing sample is solid at 200°C and practically insoluble in water (thus this sample can not contain CrO_3). XRD analysis showed that sample at the end of this stage is amorphous. Finally it seems, that when thermal decomposition is carried out in air – practically total amount of chromium passes from trivalent state through hexavalent state again to the trivalent state in Cr_2O_3.

Stage *Va*: ~200 – ~395°C, $\alpha_{TG}\cong 0.94$

$$Cr^{III}_{\sim 0.01}Cr^{VI}_{\sim 0.99}O_{\sim 2.99}\xrightarrow{200-395°C}Cr^{III}_{\sim 0.15}Cr^{VI}_{\sim 0.85}O_{\sim 2.70}(+Cr_2O_3)+O_2 \qquad (14)$$

This stage is analogous to stage *VIh*.

Stage *VIa*: ~395 – ~407°C, $\alpha_{TG}\cong 0.98$

$$Cr^{III}_{\sim 0.15}Cr^{VI}_{\sim 0.85}O_{\sim 2.70}(+Cr_2O_3)\xrightarrow{395-407°C}Cr^{III}_{\sim 0.7}Cr^{VI}_{\sim 0.3}O_{\sim 1.95}(+Cr_2O_3)+O_2 \qquad (15)$$

Stage of fast oxygen evolution, only Cr_2O_3 structure is observed. Relatively stable $Cr^{III}_{\sim 0.7}Cr^{VI}_{\sim 0.3}O_{\sim 1.95}$ phase is formed (Fig. 2). In this stage sharp exothermic DTA peak is observed and thermal effect is stronger when heating rate is greater. This effect can result from either crystallization of some Cr–O phase or molecular oxygen formation, $2O=O_2$ (in elementary act of reaction (15) atomic oxygen is formed). Nevertheless XRD analysis did not show any other phase than Cr_2O_3. On the other hand this exothermic effect is not observed in helium when rapid oxygen evolution takes place also (stage *VIIh*).

Stage *VIIa*: ~407 – ~415°C, $\alpha_{TG}\cong 0.99$

$$Cr^{III}_{\sim 0.7}Cr^{VI}_{\sim 0.3}O_{\sim 1.95}(+Cr_2O_3)\xrightarrow{407-415°C}Cr^{III}_{\sim 0.85}Cr^{VI}_{\sim 0.15}O_{\sim 1.73}(+Cr_2O_3)+O_2 \qquad (16)$$

Another stage of fast oxygen evolution. Relatively stable $Cr^{III}_{\sim 0.85}Cr^{VI}_{\sim 0.15}O_{\sim 1.73}$ phase is formed (Fig. 2). To our knowledge the relatively stable Cr–O phases of compositions $Cr^{III}_{\sim 0.7}Cr^{VI}_{\sim 0.3}O_{\sim 1.95}$ and $Cr^{III}_{\sim 0.85}Cr^{VI}_{\sim 0.15}O_{\sim 1.73}$ have never been reported before.

Stage *VIIIa*: ~415 – >450°C

$$Cr^{III}_{\sim 0.85}Cr^{VI}_{\sim 0.15}O_{\sim 1.73}(+Cr_2O_3)\xrightarrow{>415°C}Cr_2O_3+O_2 \qquad (17)$$

Conclusions

By changing conditions of the experiment we can change ratios between described above particular stages. Therefore the picture of thermal decomposition of $Cr(NO_3)_3{\cdot}9H_2O$ may sometimes appear as completely different from described above, which explains mentioned before discrepancies found in other papers. Till temperature reaches 150–180°C (stages *Vh* and *IVa*) reaction proceeds in liquid or liquid+solid phase. Therefore exact composition of intermediate compounds can not be given.

Discussed reaction can be applied for producing nonstoichiometric powder chromium oxides. For example, increasing heating rate and carrying decomposition in helium (or other inert gas) we can obtain chromium oxides of compositions from the range: $Cr^{III}_{\sim 0.07}Cr^{VI}_{\sim 0.93}O_{\sim 2.90}$–$Cr^{III}_{\sim 0.2}Cr^{VI}_{\sim 0.8}O_{\sim 2.70}$. The same can be obtained by increasing mass of the sample. When thermal decomposition is carried out in air, two other, relatively stable phases $Cr^{III}_{\sim 0.7}Cr^{VI}_{\sim 0.3}O_{\sim 1.95}$ and $Cr^{III}_{\sim 0.85}Cr^{VI}_{\sim 0.15}O_{\sim 1.73}$ from the Cr–O system can be obtained. At that moment there is no explanation why these phases were not reported for CrO_3 thermal decomposition, which is the reaction studied from tens of years.

* * *

Authors wish to acknowledge Polish State Committee for Scientific Research for financial support under project No. 9 T12D 006 16.

References

1 L. Gubrynowicz and T. Strömich, Thermochim. Acta, 115 (1987) 137.
2 I. I. Kalinichenko, A. M. Sirina and A. I. Purtov, Zh. Neorg. Khim., 19 (1974) 1547.
3 I. S. Matusevich, Zh. Prikl. Khim., 42 (1969) 1657.
4 A. Małecki, R. Gajerski, S. Łabuś and B. Prochowska-Klisch, J. Therm. Anal. Cal., 60 (2000) 17.
5 H. Schneider, M. Maciejewski, K. Köhler, A. Wokaun and A. Baiker, J. Catal., 157 (1995) 312.
6 Y. Shimizu, F. C. Lin, Y. Takao and M. Egashira, J. Am. Ceram. Soc., 81 (1998) 1633.
7 W. D. Hill Jr., Inorg. Chim. Acta, 65 (1982) L100.
8 G. C. Maiti, M. L. Kundu and S. K. Gosh, J. Indian. Chem. Soc., 52 (1975) 1119.
9 W. Xie, W. P. Pan, J. Therm. Anal. Cal., 65 (2001) 669
10 B. Małecka, E. Drożdż-Ciesla, A. Małecki, J. Therm. Anal. Cal., 68 (2002) 819
11 A. Małecki, B. Małecka, R. Gajerski and S. Łabuś, Proc. VIII Bretsznajder Seminar, 18–20 September 2002, Plock, Poland, in press.
12 Y. S. Sayi, Int. J. Mass Spectrometry, 214 (2002) 375.